Thermal Design of a Purged Cryogenic CFRP Tank and TPS Test Demonstrator for RLV

Thomas Reimer[1] and Carolin Rauh[2]
DLR, German Aerospace Center, Stuttgart, 70569, Germany

In the TRANSIENT project of DLR, critical technologies for reusable launch vehicles are investigated. One of the critical aspects identified is the structural attachment of thermal protection system surface panels to the main vehicle structure if this is a cryogenic tank at the same time. In the preceding project AKIRA it was found that the inclusion of a purging system between the cryogenic insulation on the tank and the thermal protection system reduces the required wall thickness of the insulation system considerably in the case of certain requirements. In the TRANSIENT project thermal management aspects are investigated in the case of a cryogenic CFRP fluted core tank structure, this time including a purge system within the tank structure. The thermal protection system is based on the use of ceramic matrix composite surface panels. On the tank outside, an insulation system consisting of a layer of cryogenic insulation and high-temperature insulation is installed. The investigations were done employing numerical simulations to design the required wall thicknesses of the insulation layers, determine material choices for the thermal protection system attachments and find the required parameters for the purge gas flow with regard to gas temperature and mass flow.

I. Introduction

There is the need to improve the efficiency of space transportation. As a consequence, single-use launchers are being improved but, more important, the concepts of reusable launch vehicles are developed further. In terms of the structural improvement, carbon fiber reinforced plastic (CFRP) materials are investigated to reduce the mass of the launcher structures. This is especially challenging in the case of an integral cryogenic fuel or oxidizer tank because the low temperatures and large temperature differences pose difficulties in terms of the leak-tightness of the tank.

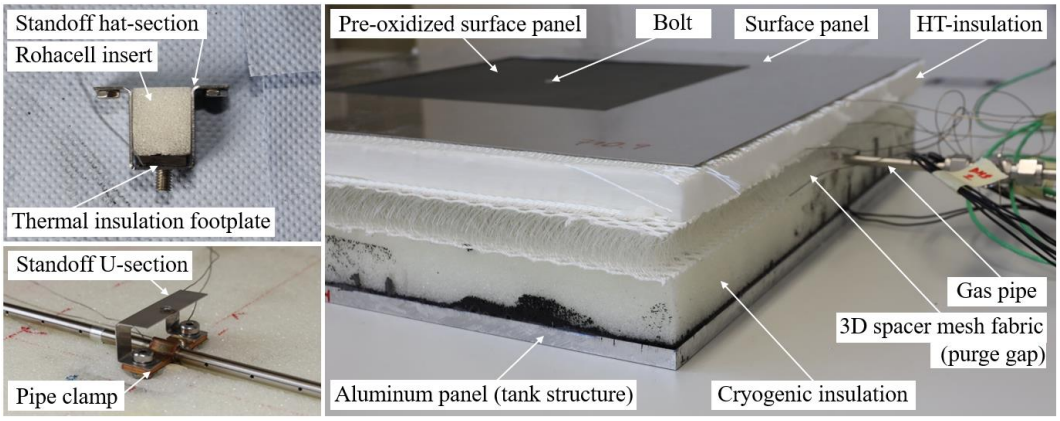

Fig. 1 Integrated Test Object from the AKIRA project.

In addition, the aim to fly a vehicle to orbit for a number of times creates the need for a thermal protection system so that the launcher survives re-entry to earth. One option for a reusable thermal protection system (TPS) is based on the

[1] Research Engineer, Department Space Systems Integration, Institute of Structures and Design, Pfaffenwaldring 38-40
[2] Research Engineer, Department Space Systems Integration, Institute of Structures and Design, Pfaffenwaldring 38-40

use of ceramic matrix composite (CMC) surface panels that are attached to the vehicle main structure via dedicated structural attachments. This type of structural attachment to the tank structure poses technical challenges in terms of thermal management. This is exacerbated in the case of a cryogenic tank and in the case of a CFRP tank.

II. General Concept of Tank Structure and Thermal Protection System

A literature review was done to review the state-of-the-art design concepts that had been considered for application as CFRP structures for launch vehicles, both in the case of single-use or reusable vehicles. One prominent example for an integrated cryogenic CFRP tank was the NASA X-33 vehicle built by Lockheed Martin [1]. It contained a multi-lobed conformal tank from CFRP honeycomb sandwich material for liquid hydrogen (LH2) which was developed up to ground testing. Another example was the DC-XA vehicle by McDonnell Douglas [2], which actually performed a number of test flights. The recent Composite Cryotank Technology Development (CCTD) project of NASA/Boeing on the development of a test demonstrator for a composite cryotank was considered the most advanced study on the topic [3]. The project was concerned about the design, analysis, manufacturing and testing of a 5.5 m diameter cryo-tank produced from CFRP material. In this project, the structure concept of the so-called fluted core was adopted for different reasons. This concept is a double-walled structure including internal, canted stiffener webs, creating separated channels (flutes) in the structure wall. It is on the one side structurally effective in terms of a high stiffness to mass ratio, like sandwich structures, but avoids some of the drawbacks of typical sandwich components including a dedicated core of foam or honeycomb with ensuing bonding issues [4]. On the other side, it also gives the possibility to control the tank environment via purging the internal channels, thus flushing leaked hydrogen gas out in a controlled way, and so avoiding safety risks.

In addition, the double-walled fluted core structure is interesting because the internal channels give the possibility to integrate a thermal management system into the structure. Thus, the fluted core design was selected as the structural concept to investigate the possible integration of the purging functionality into the structure as a kind of thermal management system. In terms of material selection, the combination of the IM7 fiber and the resin system Cycom®5320-1 from Solvay was selected in order to stick to what was described and to fabricate components out of autoclave. The principal dimensions selected for the fluted core were 60 mm channel width, 30 mm channel height and a 45° angle of the flute internal side walls. A wall thickness of 2 mm for the skins and 1 mm for the flutes was selected. For the actual hardware that was produced for the lab tests, a slightly larger spacing of 85.5 mm between the channels was chosen to achieve a bonding area of 10 mm width on the top of the stiffening webs as shown in Fig. 2.

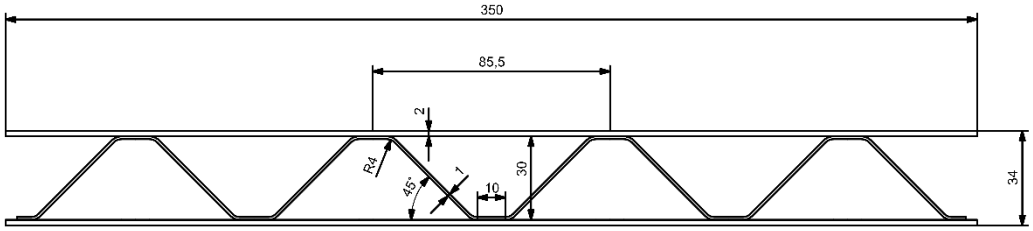

Fig. 2 Cross section of the selected fluted core geometry.

From the previous DLR project AKIRA [5], there was the baseline concept of having two layers of insulation on the outside of the tank structure. First, a dedicated cryogenic insulation for low temperature use, for which Rohacell® was selected due to the good availability and for comparison reasons with AKIRA. Second, as part of the TPS, a commercially available high-temperature fibrous ceramic insulation, (Altramat®), was placed directly under the surface panels. With regard to the structural concept of the TPS, a simplified aeroshell design was chosen, with rigid surface panels made from CMC material that are attached to the main tank structure via dedicated attachment components, hereafter called the standoffs. The surface panels are designed to be made from the CMC material C/C-SiC which DLR is producing in-house. The material is fabricated via a reactive-melt-infiltration (RMI) process, also referred to as Liquid Silicon Infiltration Process (LSI) [6].

As the focus of the project is not the detailed TPS design for a given vehicle but the understanding of the thermal management issues of a general system, some simplifications were made with regard to the level of detail of the TPS standoffs since they serve mainly as thermally representative elements. The standoff assembly consists of an upper part made of stainless steel and a lower part made of CFRP. Between the two standoff components is initially a spacer plate that can be used to tailor the thermal conductance of the complete standoff assembly. The plate was chosen to be of a low-conductivity material at first. The design was based on the approach as the one selected in the AKIRA project, with minor differences. An important consideration in designing the lower CFRP connection element was the

question of how to fix it to the tank. It was decided that it shall be bonded by adhesive to avoid the need of mechanical fastening in the fluted core, which could compromise the tightness against leakage. To ensure a good bond it was also decided that the material of choice should be CFRP for the lower part of the standoff to eliminate possible thermal expansion mismatch between standoff component and tank skin. The upper standoff element is in direct contact to the CMC surface panels which can become quite hot. A metal of good high-temperature stability is selected. In order to avoid costly high-temperature alloys, stainless steel was selected. The TPS surface panels are connected to the combination of standoff components via a metallic fastener made of Inconel 600. To keep things simple for the lab tests, a simple nut was used in the connection of the surface panels to the standoff.

III. Numerical model and results

The numerical simulations were split into two phases. At first a two-dimensional model was built to investigate the global requirements for the thickness of the two insulation layers in different cases. In a second phase a detailed 3-D model was used to determine the local temperatures around the standoff components. In terms of the purge gas flow, the simulation parameters were the temperature of the purge gas and the mass flow for both models, which was given by the convective heat transfer coefficient on the boundaries of the purged flute channels.

With regard to the applied loads, two main load cases were investigated. First a steady-state condition is looked at, which is representative of the launcher standing on the launch pad and being filled with cryogenic fuel. As the filling can last for several hours, the load case is assumed to be steady-state. Second, there is the transient heat load acting on the vehicle during the flight, which comprises both ascent and re-entry. There is a slowly increasing heat load during ascent and a short peak of high heat load during re-entry. The heat load data is derived from the trajectory of the reference vehicle SpaceLiner7 [7] and is outlined in Fig. 3.

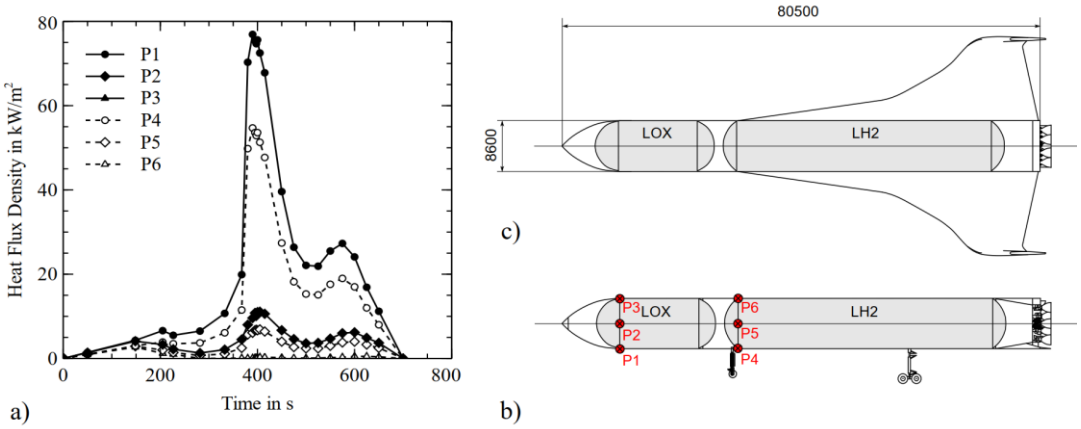

Fig. 3 Heat loads on selected positions of the SpaceLiner7 booster vehicle.

Two requirements for the design of the thickness of the insulation layers were established already during the previous work in the AKIRA project. The first requirement R1 is, that the temperature in the high-temperature insulation shall not drop below 0 °C (more exactly the dew point) to avoid condensation or freezing of humid air, thereby deteriorating the insulation performance. The second requirement R2 is that the temperature of the cryo-insulation shall stay below the maximum use temperature of the foreseen material, Rohacell, which is 170 °C.

The numerical models were built by using the commercial ANSYS Workbench software [8]. Fig. 4 shows a sketch of the model with the different material regions and the applied boundary conditions. On the inside of the fluted core structure, a constant temperature boundary condition was applied to represent the cryogenic fluid. Inside all of the fluted core channels radiation heat transfer was enabled. On the surfaces of the fluted core channels that open toward the outside of the tank structure, convective heat exchange was applied to simulate the gas purging inside those channels. It was found that a good compromise between purging effect and resulting boil-off losses can be achieved by applying the purging only in those channels that are opening to the outside of the tank, so that heat transfer into the fuel is limited but thermal control of the insulation layers is still effective. On the top of the CMC surface panel, radiative heat exchange with the environment was enabled, as well as a convective heat exchange to simulate the condition of a launcher standing vertically on the launch pad with the resulting convection along a vertical cylinder which is colder than the environment.

The type of cryogenic fluid inside the tank was either liquid oxygen or hydrogen, with a temperature of -183 °C or -253 °C, respectively. In order to obtain results that were more applicable to the planned laboratory tests, which

were to be carried out with liquid nitrogen at -196°C, further simulations were carried out with a temperature boundary condition of -183 °C, the temperature of liquid oxygen, which is almost identical to that of liquid nitrogen.

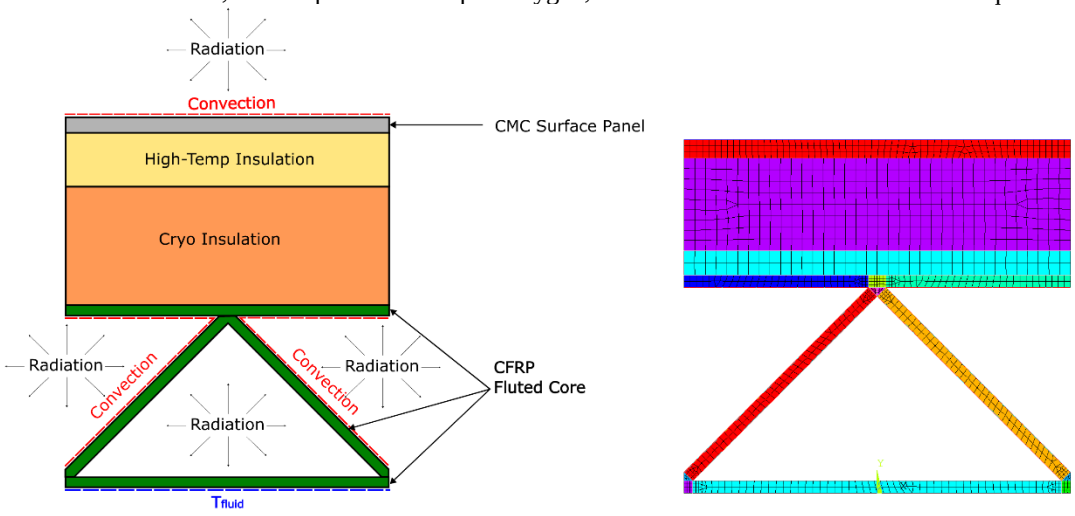

Fig. 4 Model of the structure, insulation and surface panel with boundary conditions (left) and FEM mesh (right).

A parametric study was first done to determine the influence of the purging on the resulting thickness of both cryogenic insulation and high-temperature insulation, respecting the two temperature requirements as described before. It was found that the fluted core structure without internal purging behaves almost in the same way as a simple plate due to the relatively high conductivity of the CFRP material. This is also the case for the fluted core structure having the internal volumes filled with an insulating foam material. In the case when there is no purging in the structure, the total required thickness of both insulations is 150 mm, with 135 mm of cryo-insulation and 15 mm of high-temperature insulation as shown in Fig. 5. This was comparable to the values already found in the AKIRA project, which is not surprising because the external heat loads are identical. On the right in Fig. 5 the temperature distribution of only the fluted core structure is depicted showing that there is only a small difference between the cold fluid side at -183 °C and the other side of the structure which is at -170 °C.

However, with purging enabled, it is possible to achieve a low thickness of both cryogenic and high-temperature insulation and to meet both temperature requirements R1 and R2 simultaneously during the pre-launch steady state and transient re-entry conditions. Internal purging was found to be very effective because the internal side walls of the corrugated core ensure excellent heat transfer. Thus, the wall thickness of the two insulations on top of the fluted core can be reduced to a low value, in fact, the thickness of the cryo-insulation can be reduced practically to zero if this is desired.

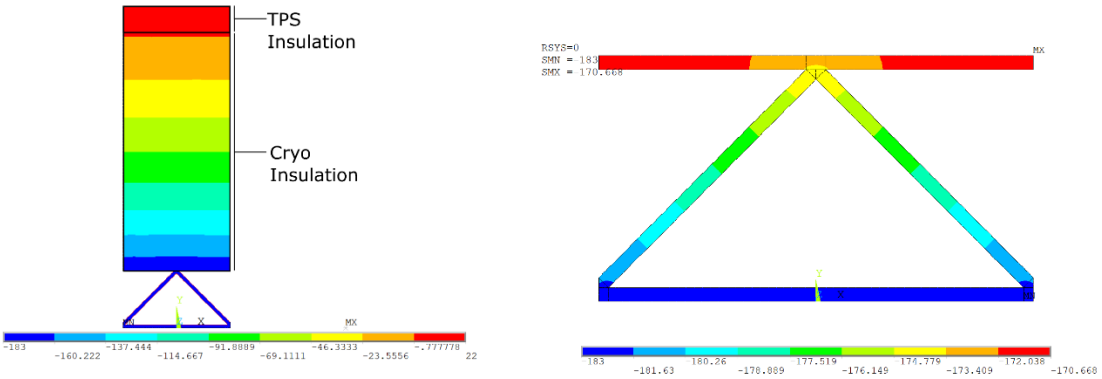

Fig. 5 Temperature distribution without purging (left) and temperature distribution in the fluted core structure (right).

The results of this parametric study are summarized in Table 1. In column one, the simulation number is given. Column two indicates whether there are one or two channel layers in the fluted core structure. Column three gives the temperature of the fluid on the inside of the fluted core. Columns four and five denounce if there is purging activated

in the respective layer. Columns six and seven show the heat transfer coefficient applied for the purging on the inside of the channels and the assumed gas temperature. Columns eight and nine give the resulting thickness values for both insulation types, first the cryo-insulation directly on the fluted core structure and then the high-temperature insulation on top. Column ten shows the temperature value at the interface between the two insulation layers. The thickness variation of the cryo-insulation was done until this temperature was 0 °C or above. Since the thickness was changed only in full millimeter steps, also negative fractions of a degree were accepted as zero. The last column shows the resulting(?) temperature on the top skin of the fluted core structure. In the following the different simulation cases are described in short. The thickness of the high-temperature TPS insulation was always kept constant at 15 mm thickness for practical reasons, which is due to availability of the commercial product and to installation issues. In addition, during the preceding AKIRA project it was found that 15 mm is enough high-temperature insulation to protect the underlying material during the time of the re-entry heat load.

Table 1 Simulation parameters and results for the 2-D study of the purging efficiency.

Sim #	FC levels	Fluid temp.	Purge upper level	Purge lower level	alpha	T gas	Thickn. cryo ins.	Thickn. TPS ins.	Temp. cryo/TPS interface	Temp. FC skin
		°C			W/m²K	°C	mm	mm	°C	°C
25	1	-183	-				135	15	-0.6	-174.3
33	1	-183	✓		10	-100	99	15	0.17	-103.3
38	1	-183	✓		20	0	4	15	0.66	-2.98
48	1	-253	✓		20	0	10	15	-0.04	-11.4
50	2	-183	-	-			55	15	-13.4	-149.9
52	2	-183	✓	✓	20	0	55	15	9.91	-0.43
54	2	-183	✓	-	20	0	0	15	-	-2.27
56	2	-183	✓	-	20	2.5	0	15	-	0.02
62	1	-183	✓		10	25	0	15	-	0.12
69	1	-253	✓		10	34	0	15	-	0.22
78	1	-253	✓		9	22	10	15	0.23	-13.4
80	1	-253	✓		5.6	21	20	15	0.29	-24.7
83	2	-183	✓		1.9	20	30	15	0.14	-29.9

Simulation #25 serves as the reference case without purging. In this case, the required thickness of the cryo-insulation became 135 mm to achieve R1 (temperature of 0 °C at the interface (I/F) between the insulations). Then, in a first step, in simulation #33, the purging was activated in the simulation with a heat transfer coefficient of 10 W/m²K and an assumed gas temperature of -100 °C, resulting in a thickness of 99 mm for the cryo-insulation.

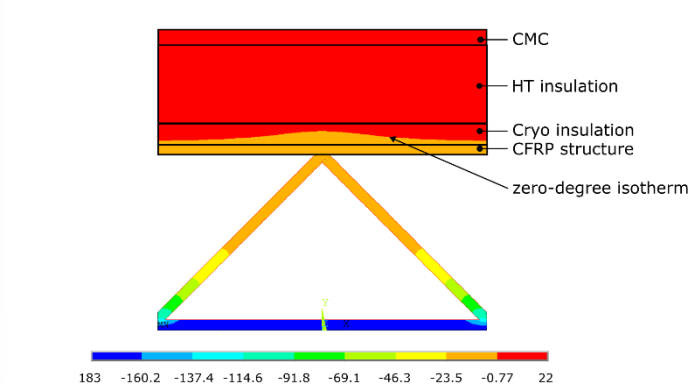

Fig. 6 Temperature distribution result of simulation #38.

Increasing the gas temperature to 0 °C in simulation #38 reduced the required thickness of the cryo-insulation to just 4 mm which is shown in Fig. 6. Simulation #48 is the comparison between liquid oxygen as the fluid and liquid hydrogen. In the case of LH2, the required thickness of the cryo-insulation increases from 4 to 10 mm.
Simulations #50 to #56 describe the case where the fluted core structure consists of two layers of channels on top of each other. Simulation #50 is again the reference case without purging. The addition of a second layer of flute channels reduces the required thickness of the cryo-insulation from 135 mm to 55 mm. When the purging is activated in both layers, as it is in simulation #52, and the thickness of the cryo-insulation is kept at 55 mm, the I/F temperature between the insulations increases to 9.91 °C and the temperature on the skin of the fluted core structure is practically at 0 °C. If the purging is restricted to the upper level, and the cryo-insulation is completely omitted, the temperature at the fluted core skin is just -2.2 °C. If the R1 requirement is to be kept there too without cryo-insulation, it can be achieved via increasing the gas temperature to 2.5 °C.

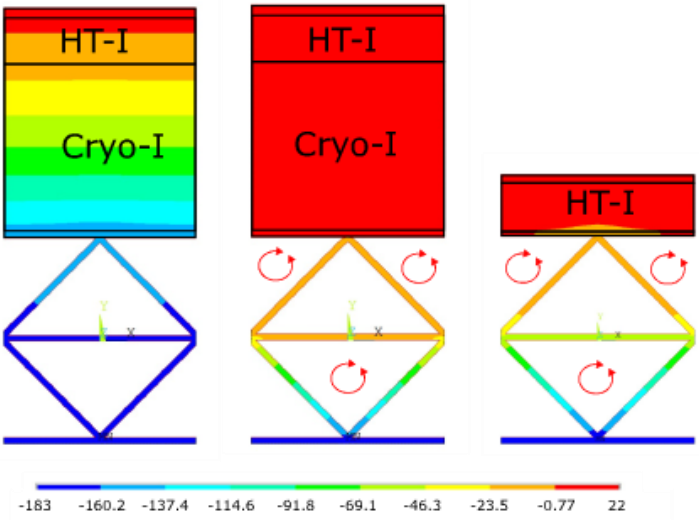

Fig. 7 Temperature distribution with double-layer fluted core for simulations #50, #52 and #54 (left to right).

The simulations #62 and the following ones aimed at investigating different settings for the heat transfer coefficient and the purge gas temperature for the two different types of fluid (and thus temperature) in the tank. Simulation #62 is for liquid oxygen (LOX) boundary condition in the tank and zero thickness for the cryo-insulation. The R1 condition can be achieved with a heat transfer coefficient of 10 W/m²K in combination with a gas temperature of 25 °C. In comparison, simulation #69 is the case with LH2 and also zero thickness of the cryo-insulation and the same value of 10 W/m²K for the heat transfer coefficient. In this case, a gas temperature of 34 °C is sufficient to achieve the R1 objective.
Simulations #78 and #80 investigate the question which combinations of heat transfer coefficient and gas temperature are necessary if a certain thickness of cryo-insulation is fixed. Simulation #78 looks at the case of LH2 and 10 mm cryo-insulation, for which the heat transfer coefficient of 9 W/m²K in combination with a gas temperature of 22 °C satisfy the requirement R1. In simulation #80, the thickness of the cryo-insulation is doubled to 20 mm and consequently, the required heat transfer coefficient decreases to 5.6 W/m²K whereas the gas temperature stays almost constant at 21 °C.
Simulation #83 goes back to LOX for the fluid and looks at a two-layered fluted core again. It assumes a fixed value of 30 mm for the cryo insulation, 15 mm for the TPS insulation, and gives a result of 1.9 W/m²K for the heat transfer coefficient and a gas temperature of 20 °C.
These results in terms of insulation thickness and purge gas parameters were taken as guidelines for further investigations of a more detailed 3D model of the actual test hardware, including surface panel attachment structures, which is going to be discussed in the following. Since the planned lab tests with the Integrated Test Object (ITO) were foreseen to be done with liquid nitrogen, the 3D simulations focused on the LOX case because of the similar temperature level.
The price to pay for the reduction of the insulation thickness via active purging between tank and the external insulations is an increased heat flow into the tank, i.e. into the fuel, which leads to increased boil-off losses. Values for the heat flow into the tank were also determined in the simulations discussed above. As can be expected, the heat flow into the tank increases when the thickness of the outward layers of insulation is reduced. A comparison is made

between three simulations, each using LH2 as the fluid and a fixed value of 15 mm for the TPS insulation. Then for simulation #69, the thickness of the cryo-insulation is set to zero, whereas for simulation #78 it is set to 10 mm and for simulation #80 it is set to 20 mm. The purging parameters are selected in such a way that at the interface between cryo-insulation and TPS insulation the R1 requirement is satisfied, i.e. there is 0 °C. The results presented in Table 2 show that the heat flow into the tank is between 1.3 and 1.6 kW/m² and that by increasing the thickness of cryo-insulation on top of the fluted core structure, the heat flow into the tank decreases. In addition, the value for the heat flow into the tank is given for the case of LOX in the tank and no cryo-insulation on the structure. It is somewhat lower than for LH2, at a value of 1.2 kW/m².

Table 2. Heat flow into the tank due to purging, depending on insulation thickness for single-layer structures.

Simulation #	Tank temp.	Cryo-insulation thickness	TPS insulation thickness	alpha	Purge gas temperature	Heat flow into the tank
	°C	mm	mm	W/m²K	°C	W/m²
69	-253	0	15	10	34	1616
78	-253	10	15	9	22	1479
80	-253	20	15	5.6	21	1330
62	-183	0	15	10	25	1192

The lowest values for the heat flow into the tank were achieved with the double-layered fluted core structure. In Table 3 the results for some of those cases are given, with the direct comparison to simulation #80 (single-layer) listed under simulation #81 for the double layer case and LH2 as the fluid. The heat flow is just 453 W/m² compared to 1330 W/m² for simulation #80.

Table 3. Heat flow in the tank due to purging, depending on insulation thickness for double-layer structures.

Simulation #	Tank temp.	Cryo insulation thickness	TPS insulation thickness	alpha	Purge gas temperature	Heat flow into the tank
	°C	mm	mm	W/m²K	°C	W/m²
81	-253	20	15	3.2	21	453
82	-253	30	15	2.6	21	429
83	-183	30	15	1.9	20	295

As a result of these simulations, thickness values of 30 mm for the cryogenic insulation and 25 mm for the high-temperature insulation were selected along with purging parameters for further detailed simulations of the local temperature field in the vicinity of the standoff components. The value of 30 mm thickness for the cryo-insulation was selected to limit the amount of heat flow into the tank. The increase of the TPS insulation thickness was made because it was expected that the attachment structures would act as thermal shorts between hot surface panels and the CFRP structure. A 3D model shown in Fig. 8 was built to investigate the local temperatures around the standoff components. The applied loads correspond to the position P1 in Fig. 3, which is the most forward position on the windward side of the LOX tank.

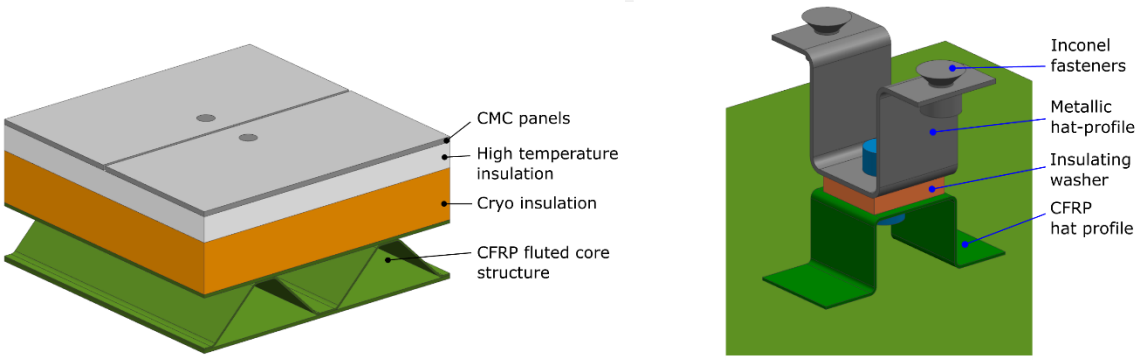

Fig. 8 Detailed 3D model of fluted core and standoff components with insulation (left), without insulation (right).

First, the steady-state conditions were simulated to see whether the R1 requirement for the TPS insulation can be achieved. With the thicknesses of 30 mm and 25 mm for both insulations, the R1 condition could be met, except for a small region in the immediate surrounding of the standoff which was considered as acceptable. The purging parameters were 10 W/m²K for the heat transfer coefficient and 20 °C for the gas temperature. In Fig. 9 on the left, a side view is shown with the zero degree Celsius isotherm and on the right, there is the top view on the interface between TPS insulation and cryo-insulation, showing the small region in the standoff vicinity where the temperature is below 0 °C.

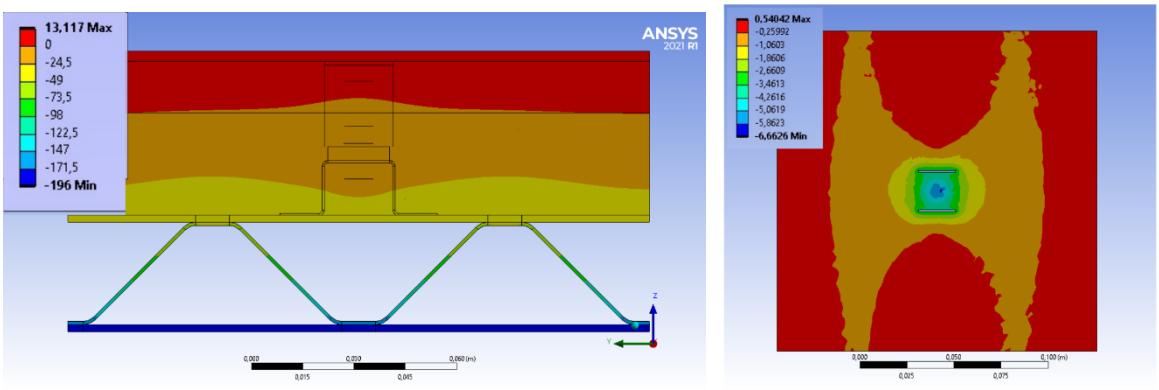

Fig. 9. Steady-state condition of initial standoff configuration.

However, the transient simulation results for the configuration obtained with the dimensions of 30 mm cryo-insulation and 25 TPS insulation showed exceedingly high temperatures during the re-entry case for the cryo-insulation around the lower part of the standoff. The transient temperature graphs of the simulation with the initial standoff configuration are presented in Fig. 10.

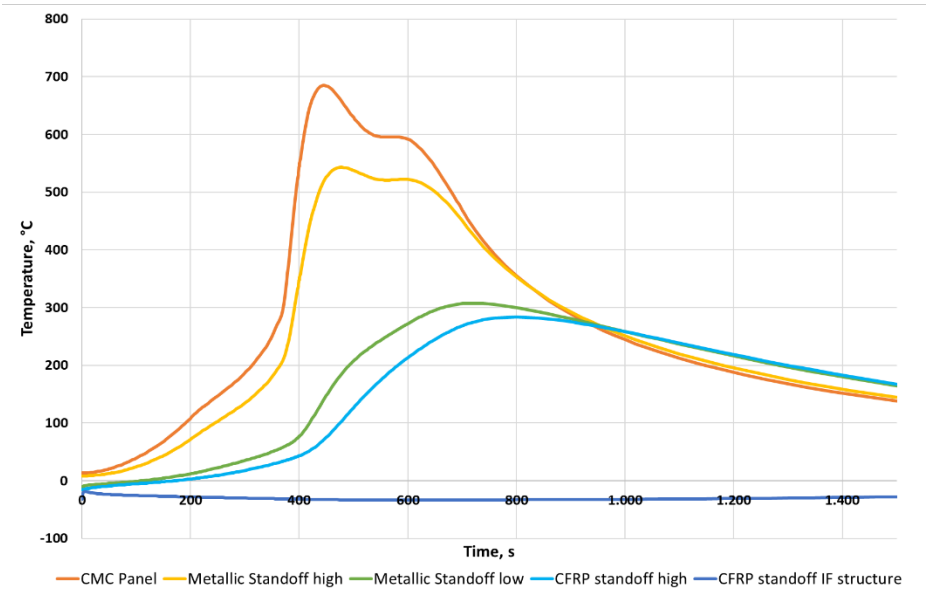

Fig. 10 Transient temperatures obtained with the 3D model; standoff in initial configuration.

The lower part of the metallic standoff component, which is corresponding to the upper boundary of the cryo-insulation, reaches over 300 °C. Also, the temperature for the lower CFRP standoff part itself was too high with 280 °C, as shown in Fig. 11. Because the maximum use temperature of the cryo-insulation is 170 °C and that for the CFRP material 150 °C, the simulation result was very unfavorable. It was recognized that the problem was due to the insulation plate between the two standoff parts limiting the thermal conductance between the standoff parts. The reason for having the insulation washer plate there, was the consideration that it would help during the steady-state phase to keep the temperatures in the TPS insulation from getting too low.

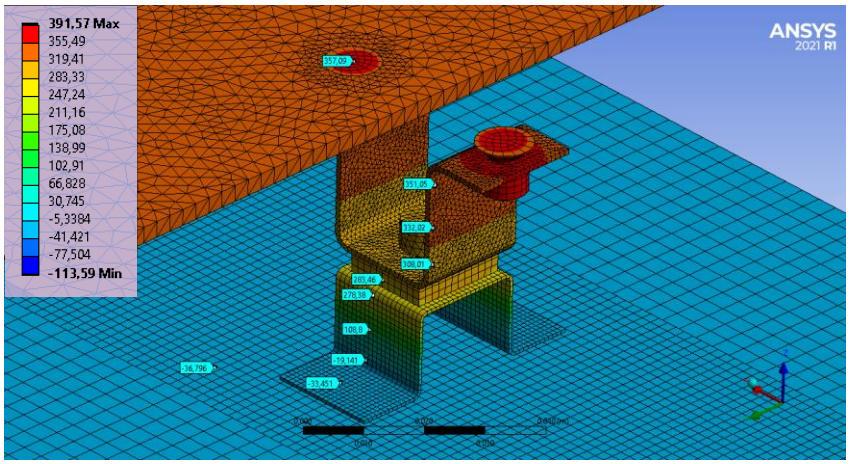

Fig. 11 Temperatures for the standoff components in the initial configuration at the time of 800 s when the temperature maximum of the CFRP standoff component is reached.

Because it was counter-productive to insulate the upper and lower standoff component from each other, it was investigated if a change to aluminum for the material of the washer plate would improve the situation. That was the case, and, it was also found that if the material of the lower CFRP standoff component was changed to aluminum, the temperatures at the top boundary of the cryo-insulation went down as desired. Therefore, as a consequence, a re-design of the standoff concept was done. The lower CFRP standoff was kept due to manufacturing and thermal compliance considerations. Instead, an additional aluminum component was introduced which replaced the insulating washer plate. It had the shape of a U-profile and was put above the CFRP component, opening downwards and extending almost to the bottom of the CFRP standoff component just above the fluted core facesheet. The objective was to establish a very good thermal contact between the cold fluted core facesheet and the metallic standoff component to help in cooling the standoff components during the re-entry phase. In Fig. 12 the initial standoff assembly is shown on the left, whereas on the right the re-designed standoff assembly is shown.

Fig. 12 Re-design of the standoff assembly – old (left) vs. new (right).

During the re-entry phase, the heat which is transferred down the upper standoff component needs to be counteracted by close coupling to the low temperatures of the tank. By re-designing the standoff assembly this goal could be achieved. During the steady-state ground phase, when the purging is active, this design is also good because the purging is forcing the insulation layers on top of the tank structure practically into the same temperature condition.
The temperature distribution for the steady-state simulation with the same purge gas parameters as for the previous variant is shown in a side view in Fig. 13. It can be noted, that with the same purge parameters, the situation is slightly worse in comparison to Fig. 9 because the R1 requirement is not fully achieved. The temperatures at the interface between cryo and high-temperature insulation are around -15 °C. However, it was concluded that via an adjustment of the purge parameters it should be possible that the R1 requirement will be achieved.

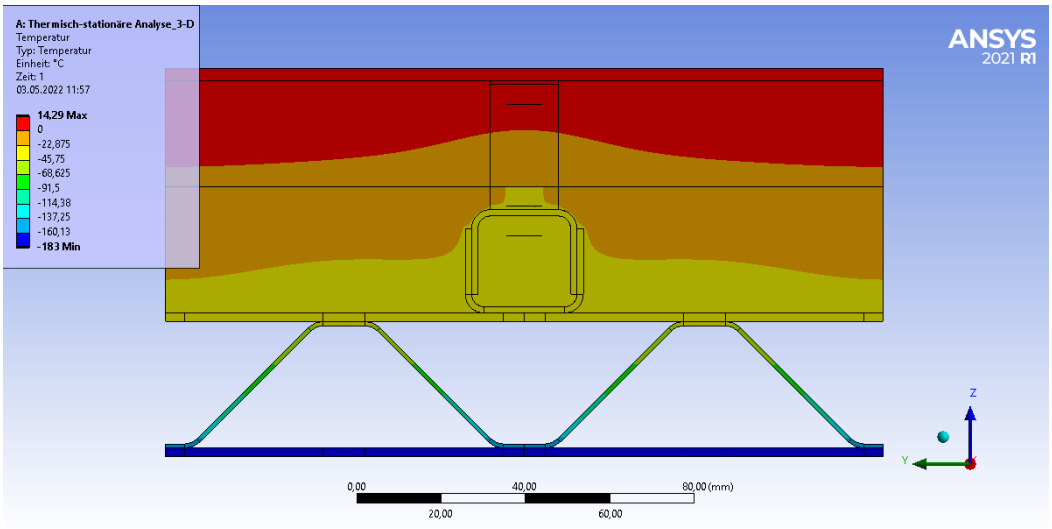

Fig. 13 Steady-state temperature distribution with the re-designed standoff assembly.

The situation in the transient simulation is noticeably better with this type of standoff configuration. In Fig. 14, the temperature distribution in the standoff components is shown at the time of 725 s, which corresponds to the temperature maximum of the lower part of the metallic standoff component. Various sample points show the values at selected positions of importance. Due to the fact that now there is the intermediate aluminum component which is a very good conductor, the temperatures of both aluminum part and of the CFRP standoff component are very close together and there is not much difference between upper and lower regions. It can be noted, that at the lower end of the metallic standoff, which is the critical region for the cryo-insulation, the temperature is now 151 °C, which is below the acceptable limit of 170 °C for the cryo-insulation. With regard to the CFRP standoff component, the temperatures are really low with 37 °C at the upper edge of the CFRP component. Results were thus fully acceptable in the re-entry case.

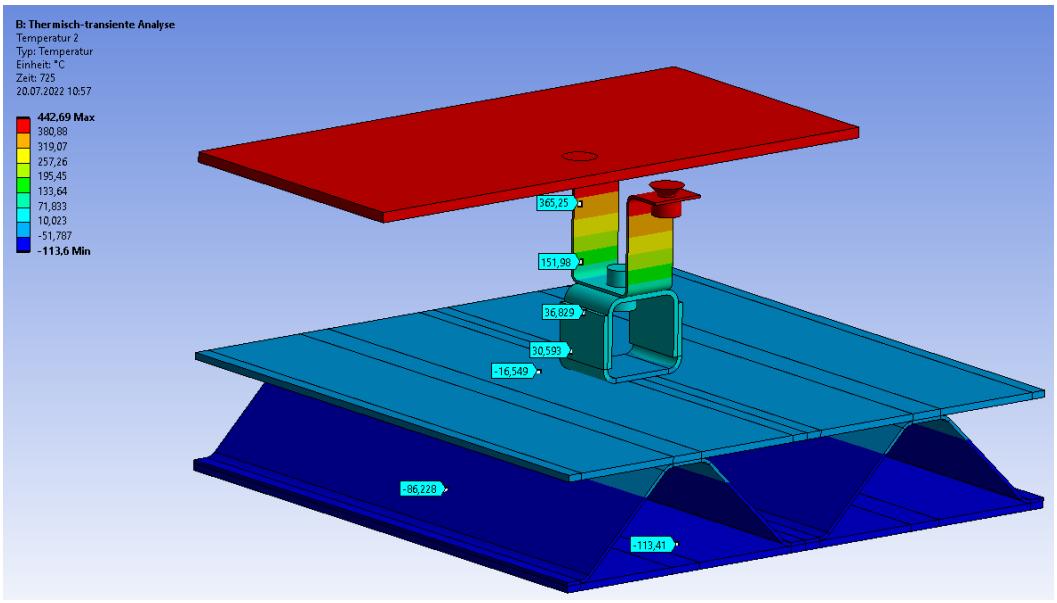

Fig. 14 Maximum standoff temperatures with the re-designed standoff assembly during re-entry.

The simulation results were regarded as a justification to go ahead with the design and fabrication of the actual ITO test hardware that was supposed to be tested in a combined thermal-mechanical test environment, the THERMEX

facility in DLR Braunschweig. The hardware design and fabrication up to the full assembly of the ITO hardware and installation in the THERMEX facility is described in [9].

IV. Conclusion

An investigation was carried out on the thermal behavior of a simplified assembly of cryogenic tank and TPS of a future re-usable launch vehicle. Two aspects were considered in more detail. First, it was investigated if the inclusion of a purging function into the fluted core CFRP tank structure during steady-state conditions prior to launch can be useful and effective in reducing the overall insulation layer thickness. Second, special attention was given to the issue of the TPS surface panel fixations being thermal shorts, and how this can be handled to keep temperatures below maximum allowable values for the selected components. It was shown that the inclusion of the purging function into the channels of the fluted core tank structure is effective, but it comes along with additional heat transfer into the cryogenic fluid, leading to increased boil-off rates. Boil-off rates were determined and acceptable values have to be defined by system level engineering. Regarding the design of the TPS attachment components between surface panels and the CFRP tank, it was found that a good thermal coupling between surface panels and tank is beneficial for the re-entry situation when the attachments act as thermal shorts, so that the maximum material use temperatures could be respected. A solution was found that gives good results for both load cases, the steady-state pre-launch case and the transient re-entry phase.

References

[1] Cook, S. A., "The Reusable Launch Vehicle Technology Program and the X-33 Advanced Technology Demonstrator," *AIAA Aerospace Plane and Hypersonics Technology Conference*, AIAA, Chattanooga, TN, 1995.

[2] Dumbacher, D., "Results of the DC-XA program," *AIAA Space Programs and Technologies Conference*, Huntsville, AL, 1996

[3] McCarville, D. A., Guzman, J. C., Dillon, A. K., Jackson, J. R., and Birkland, J. O., "Design, Manufacture and Test of Cryotank Components," Comprehensive Composite Materials II, Vol.3, 2017 doi:10.1016/B978-0-12-803581-8.09958-6

[4] Schultz, M. R., Oremont, L., Guzman, J. C., McCarville, D., Rose, C. A., and Hilburger, M. W., "Compression Behavior of Fluted-Core Composite Panels," *AIAA Structures, Structural Dynamics, and Materials Conference*, Denver, CO, 2011

[5] Reimer, T., Rauh, C., Di Martino, G., and Sippel, M., "Thermal investigation of a purged insulation system for a reusable cryogenic tank," *Journal of Spacecraft and Rockets*, Vol. 59, No. 4, 2022, pp. 1205-1213. doi: 10.2514/1.A35252

[6] Krenkel, W., and Kochendörfer, R.,"The LSI Process – A Cost Effective Processing Technique for Ceramic Matrix Composites," Proceedings of the International Conference on Advanced Materials, Int. Conf. on Advanced Materials, Beijing, China, 1996

[7] Sippel, M., VAlluchi, C., Bussler, L., Kopp, A., Garbvers, N., Stappert, S., Krummen, S., and Wilken, J., "SpaceLiner Concept as Catalyst for Advanced Hypersonic Vehicles Research," 7th European Conference for Aeronautics and Space Siences (EUCASS) 2017, EUCASS association, Milan, Italy, 2017

[8] Ansys® Academic Research Mechanical, Release 2021R1

[9] Rauh, C. and Reimer, T., "Manufacturing and Testing of a Purged Thermal Insulation Concept for Reusable CFRP Cryotanks," *25th AIAA International Space Planes and Hypersonic Systems and Technologies Conference* (to be published), AIAA, 2023.